THE TOROIDAL POROUS PLATE: A NEW METHOD TO FACILITATE WATERFLOODING

Christopher H. Pentland[1*], Rehab M. El-Maghraby[2], Stefan Iglauer[3] and Martin J. Blunt[4]
[1]Shell Global Solutions International B.V., The Netherlands.
[2]Suez University, Egypt. [3]Curtin University, Perth, Australia.
[4]Imperial College London, United Kingdom.

This paper was prepared for presentation at the International Symposium of the Society of Core Analysts held in Avignon, France, 8-11 September, 2014

ABSTRACT

We present a modified porous plate core flooding apparatus where the porous plate has a hole drilled through its centre resulting in a toroid shape similar to a British Polo peppermint, an American Life Savers candy, or a doughnut. The apparatus allows primary drainage and imbibition (water flood) flow sequences to take place sequentially, without the need to remove the sample. During primary drainage the modified porous plate behaves in the same way as a solid, unmodified, porous plate. The method used to isolate the water flood flow line passing through the centre of the porous plate is effective and the plate can withstand capillary pressures up to 5 bar. During water flooding the porous plate is effectively bypassed, with the pressure drop recorded consistent with that across the core-plug alone.

We use this new apparatus to measure the relationship between initial and residual non-wetting phase saturations. Sandstone and carbonate rocks are investigated for both decane-brine and CO_2-brine fluid systems at elevated temperatures and pressures. The challenges of effectively sealing the hole through the porous plate during drainage are discussed and additional suggestions for future improvements to the design are proposed.

INTRODUCTION

Many special core analysis studies focus on the imbibition of water into a core-plug initially containing water and oil or gas. These include imbibition relative permeability, resistivity and capillary pressure measurements. Reliably performing such experiments depends in part on our ability to accurately and reproducibly attain the correct initial saturations within the core-plug, a step which requires a primary drainage flow sequence to be performed.

Typically the porous plate or centrifuge methods are used for the primary drainage flow sequence. A core 100% saturated with water is used and some of the water is displaced by the invasion of oil or gas. Other methods can also be used, such as evaporating the water, or displacement with the unsteady or steady-state methods.

Once the desired initial ratio of water and oil or gas is achieved the subsequent imbibition flow sequence can commence. This can pose an experimental challenge as the apparatus

used for primary drainage may be different to the apparatus used for imbibition; requiring the transfer of the core-plug. Such a step can result in changes to: the saturations (for example by air entering the sample); the mass of the core (grains falling off during handling); and the phase compositions (if live crude or gases are used at elevated temperatures and pressures and the system is depressurised).

The steps and associated challenges outlined above were the motivation for the development of a modified Hassler type flow cell (Hassler, 1944) for use in decane-brine and CO_2-brine experiments at elevated temperatures and pressures. Especially in the case of the CO_2 experiments depressurising the apparatus after primary drainage and moving the core-plug was out of the question. The new flow cell incorporated a porous plate for use in the primary drainage initialisation, but this porous plate could be bypassed during subsequent imbibition. The goal of the experiments was to measure the relationship between initial and residual saturations to quantify the importance of residual trapping in subsurface applications.

EXPERIMENTAL EQUIPMENT AND PROCEDURES

Experiments were performed on Berea sandstone (porosity = 0.22; brine permeability = 4.6×10^{-13} m^2 (466 mD); diameter = 0.0385 m; length = 0.0753 m) and Indiana limestone (porosity = 0.20; brine permeability = 2.4×10^{-13} m^2 (243 mD); diameter = 0.0378 m; length = 0.0765 m). Experiments were performed at conditions representative of subsurface formations – 50 to 70 °C and 4.2 to 9.0 MPa. The aqueous phase was aqueous 5wt.% sodium chloride, 1wt.% potassium chloride synthetic brine, which in the case of the CO_2 experiments was saturated with CO_2 using a stirred reactor (El-Maghraby et al., 2012). The different experiments and their associated thermo physical conditions are summarised in Table 1.

Table 1. Thermo-physical conditions and estimated non-wetting phase properties.

Experiment	Temperature (°C)	Pressure (MPa)	Decane or CO_2 Density ($kg \cdot m^{-3}$)	Decane or CO_2 Viscosity ($Pa \cdot s$)	Interfacial Tension ($N \cdot m^{-1}$)
Berea (decane-brine)	70	9	700 [a]	5.5×10^{-4} [b]	48.3×10^{-3} [c]
Berea (CO_2-brine)	70	9	208 [d]	2.1×10^{-5} [e]	36.0×10^{-3} [f]
Indiana (CO_2-brine)	50	9	291 [d]	2.7×10^{-5} [e]	33.0×10^{-3} [f]
Indiana (CO_2-brine)	50	4.2	84 [d]	1.7×10^{-5} [e]	46.0×10^{-3} [f]

[a] (Banipal et al., 1991) [b] (Lee and Ellington, 1965) [c] (Zeppieri et al., 2001)
[d] (Span and Wagner, 1996) [e] (Fenghour et al., 1998)
[f] (Chalbaud et al., 2009; Chiquet et al., 2007)

The flow cell contained the core-plug and the modified porous plate positioned together as shown in Figure 1. All wetted parts were made of C276 alloy (Hastelloy®), herein referred to as steel. The ceramic (aluminium silicate) porous plate (Weatherford Laboratories, Stavanger, Norway) was modified by drilling a hole through its centre, through which a 1/8 inch (0.3175 cm) steel flow line could pass. Two further larger diameter recesses were drilled into either side of the porous plate to house small rubber (Viton®) o-rings. These o-rings prevented fluids passing in-between the steel flow line

and the porous plate. We found Viton® performed well when exposed to CO_2 and effective sealing was achieved. Our initial design used only one o-ring on one side of the porous plate but this was later modified to allow two o-rings to be used, one on each side. This modification was made to provide some redundancy in the design in case one o-ring failed.

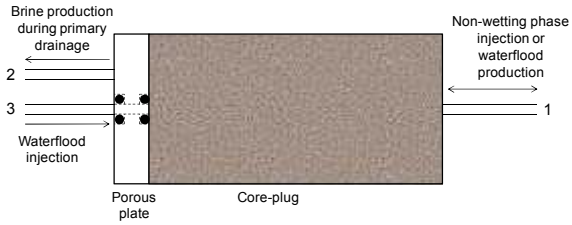

Figure 1. The modified porous plate is positioned at one end of the core-plug. Injection and production of phases is achieved using flow lines 1 through 3, different combinations of which are used in different flow sequences, as described in the text.

The modified porous plate was fitted onto the end of a steel platen. The platen had two flow lines passing through it: one through the centre that ultimately passed through the porous plate; and a second that terminated at the platen face, flush with the back side of the porous plate. This face of the platen had some grooves cut into its surface to aid the collection and production of water. Figure 2 shows the platen and porous plate configuration in further detail. The core-plug and platen were surrounded by a Viton sleeve which allowed an axial confining pressure to be applied when the assembly was fitted within the modified Hassler cell.

Figure 2. The modified porous plate is attached to the end of a steel platen which houses the two flow lines. Rubber o-rings form a seal in-between the porous plate and the central steel flow line preventing the bypassing of fluids.

The flooding sequences used different combinations of the three flow lines shown in Figure 1:

1. **Primary Drainage**
   - Non-wetting phase injected through flow line 1
   - Wetting phase produced through flow line 2
   - Flow line 3 closed with a valve

   During primary drainage the flow line that passed through the centre of the modified porous plate was closed using a valve. The apparatus functioned like a conventional (un-modified) porous plate apparatus with the non-wetting phase injected at one end and the wetting phase produced at the opposite end. The non-wetting phase is unable to enter the low permeability porous plate due to capillary entry pressure constraints. The phase pressures and injection rates were controlled with high precision syringe pumps (Teledyne ISCO 500D & 1000D, Lincoln, NE,

USA) which operated in constant pressure mode but with additional rate constraints to ensure very slow capillary controlled injection of the non-wetting phase (the capillary number (N_{cap}) was in the range $10^{-10} < N_{cap} < 10^{-11}$).

2. **Waterflooding**
   - Wetting phase injected through flow line 3
   - Production of both phases through flow line 1
   - Flow line 2 closed with a valve

   During water flooding the flow line that bypassed the porous plate (3) was opened and used to inject water into the sample. The water and oil or gas were produced from the opposite end through flow line 1. Five pore volumes of water were injected through the sample at a rate representative of field conditions (in the range $10^{-7} < N_{cap} < 10^{-5}$).

The core-plug initial saturations after primary drainage were determined based on a volume balance of the injected and produced phases. After water flooding the residual decane saturations were measured by mass balance and the residual CO_2 saturations by an isothermal depressurisation of the trapped CO_2, as described previously by Suekane et al., (2008).

RESULTS & DISCUSSION

During primary drainage the pump volumes and the differential pressure across the core-plug were recorded automatically every 5 seconds. Figure 3 shows the effluent pump volume versus time for three Berea sandstone and three Indiana limestone experiments. The differential pressure applied was 3.0, 1.6, and 0.83 bars for Berea samples 1 through 3, and 3.5, 2.8 and 0.79 bars for Indiana samples 1 through 3 respectively. The data shows that the porous plate was impervious to the non-wetting phase: for a constant applied differential pressure a finite volume of water was displaced from the sample. Towards the end of primary drainage the production rate declined, eventually reaching zero once no more water could be displaced for the applied capillary pressure. The system was then in capillary equilibrium; the porous plate was an effective barrier to the non-wetting phase and there was no more flow. If the porous plate had failed then the effluent pump would have continued to increase in volume as both water and non-wetting phase were produced.

After primary drainage the samples were water flooded. The differential pressure data was consistent with that expected from an unsteady-state imbibition experiment across the core-plug in the presence of a residual non-wetting phase (effective permeabilities: 4.96×10^{-14} to 2.98×10^{-13} m^2 (50 to 300 mD) for Berea sandstone). If the imbibing water had also flown through the low permeability porous plate then significantly lower permeabilities would have been measured (the absolute permeability of the porous plate was 1.23×10^{-16} m^2 (125 μD)). The data therefore indicates that the porous plate had been effectively bypassed by using the centre flow line. The maximum residual

saturations was 0.366 for Berea sandstone and 0.237 for Indiana limestone, as reported previously (El-Maghraby and Blunt, 2013; Pentland et al., 2011).

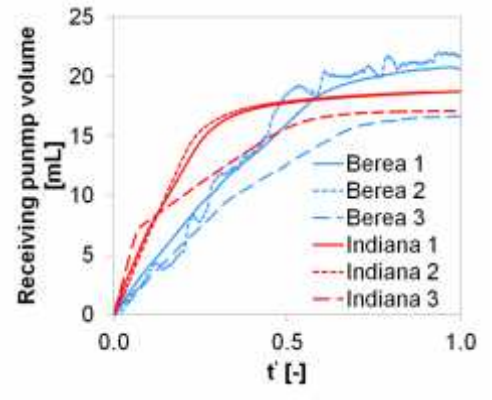

Figure 3. Receiving pump volumes versus normalised time (t') for primary drainage displacements in Berea sandstone and Indiana limestone where a finite volume is produced from the core-plug under the application of a constant capillary pressure. The time is normalised by dividing by the total duration of the displacement (20.2, 60.5 and 138.0 hours for experiments Berea 1 through 3, and 46.1, 47.6 and 73.4 hours for experiments Indiana 1 through 3 respectively).

There are details of the modified porous plate design that could be further improved. During water flooding the displacement might be affected by the single point source of brine, this effect could be minimised by engraving flow distribution channels onto the face of the porous plate, as illustrated in Figure 4. Furthermore the unsteady state water flood will result in a non-homogeneous saturation profile within the core-plug due to the capillary end effect phenomena. The use of in-situ saturation monitoring techniques would help account for this effect.

Figure 4. The porous plate could be modified further by the inclusion of flow distribution channels, allowing injection water to access a greater fraction of the core-plug cross section.

CONCLUSION

The presented modified porous plate design allows drainage and imbibition flow sequences to be performed within a single apparatus. The apparatus combines the advantages of performing drainage with the porous plate method (capillary controlled uniform initial saturation) and water flooding with the unsteady-state displacement method. Since the core is not removed in-between displacements the initial saturation is not disturbed and the possibility for core damage is minimised. The experimental data show that the hole in the centre of the porous plate is not a leak pathway for the non-wetting phase in drainage, and that the porous plate is effectively bypassed during water flooding.

ACKNOWLEDGEMENTS

This study was performed from 2007 to 2012 at Imperial College London. The authors would like to acknowledge the contribution of Andrew Cable of Weatherford

Laboratories, Winfrith, U.K. who initially suggested we test a modified porous plate method. The authors acknowledge the technical support of Graham Nash and Alexander Toth. The authors would like to acknowledge the funding of Shell under the Grand Challenge on Clean Fossil Fuels and support from the Qatar Carbonates and Carbon Storage Research Centre funded jointly by Qatar Petroleum, Shell and the Qatar Science & Technology Park.

REFERENCES

Banipal, T., Garg, S., Ahluwalia, J., 1991. Heat capacities and densities of liquid -octane, -nonane, -decane, and -hexadecane at temperatures from 318.15 K to 373.15 K and at pressures up to 10 MPa. The Journal of Chemical Thermodynamics 23, 923–931. doi:10.1016/S0021-9614(05)80173-9

Chalbaud, C., Robin, M., Lombard, J., Martin, F., Egermann, P., Bertin, H., 2009. Interfacial tension measurements and wettability evaluation for geological CO2 storage. Advances in Water Resources 32, 98–109. doi:10.1016/j.advwatres.2008.10.012

Chiquet, P., Broseta, D., Thibeau, S., 2007. Wettability alteration of caprock minerals by carbon dioxide. Geofluids 7, 112–122. doi:10.1111/j.1468-8123.2007.00168.x

El-Maghraby, R.M., Blunt, M.J., 2013. Residual CO2 Trapping in Indiana Limestone. Environ. Sci. Technol. 47, 227–233. doi:10.1021/es304166u

El-Maghraby, R.M., Pentland, C.H., Iglauer, S., Blunt, M.J., 2012. A fast method to equilibrate carbon dioxide with brine at high pressure and elevated temperature including solubility measurements. The Journal of Supercritical Fluids 62, 55–59. doi:10.1016/j.supflu.2011.11.002

Fenghour, A., Wakeham, W.A., Vesovic, V., 1998. The Viscosity of Carbon Dioxide. J. Phys. Chem. Ref. Data 27, 31. doi:10.1063/1.556013

Hassler, G.L., 1944. Method and apparatus for permeability measurements. US2345935 A.

Lee, A.L., Ellington, R.T., 1965. Viscosity of n-Decane in the Liquid Phase. J. Chem. Eng. Data 10, 346–348. doi:10.1021/je60027a013

Pentland, C.H., El-Maghraby, R., Iglauer, S., Blunt, M.J., 2011. Measurements of the capillary trapping of super-critical carbon dioxide in Berea sandstone. Geophys. Res. Lett. 38, L06401. doi:10.1029/2011GL046683

Span, R., Wagner, W., 1996. A New Equation of State for Carbon Dioxide Covering the Fluid Region from the Triple-Point Temperature to 1100 K at Pressures up to 800 MPa. J. Phys. Chem. Ref. Data 25, 1509–1596.

Suekane, T., Nobuso, T., Hirai, S., Kiyota, M., 2008. Geological storage of carbon dioxide by residual gas and solubility trapping. International Journal of Greenhouse Gas Control 2, 58–64. doi:10.1016/S1750-5836(07)00096-5

Zeppieri, S., Rodríguez, J., López de Ramos, A.L., 2001. Interfacial Tension of Alkane + Water Systems†. Journal of Chemical & Engineering Data 46, 1086–1088. doi:10.1021/je000245r